Improved flood forecasting using geomorphic unit hydrograph based on spatially distributed velocity field

Wen-chuan Wang, Yan-wei Zhao, Kwok-wing Chau, Dong-mei Xu and Chang-jun Liu

ABSTRACT

This paper presents an energy model for determining the overland flow velocity in order to improve the low accuracy problem in flow concentration simulation. It furnishes a novel idea for studying flow concentration in ungauged basins. The model can be widely applied in analysis of spatial velocity field, extraction of instantaneous geomorphic unit hydrograph and development of distributed hydrological model. A distributed flood-forecasting model is constructed for Lianyuan Basin in Hunan Province of China. In the proposed method, gravitational potential energy is transformed into kinetic energy via an analysis of energy distribution of water particles in the basin. Based on the kinetic energy equation, the overland flow velocity simulating the geomorphic unit hydrograph is computed. Rainfall-runoff simulation is then performed by integrating with runoff yield and concentration model. Results indicate that the model based on energy conversion leads to more accurate results. The model has the following advantages: firstly, the spatial distribution of the velocity field is appropriate; secondly, the model has only one parameter, which is easily determined; and finally, flow velocity results can be used for the computation of river network flow concentration.

Key words | distributed hydrological model, flood forecasting, geomorphic unit hydrograph, hydrodynamic energy, spatially distributed velocity field

Wen-chuan Wang (corresponding author)
Yan-wei Zhao
Dong-mei Xu
College of Water Resources, Henan Key Laboratory of Water Resources Conservation and Intensive Utilization in the Yellow River Basin,
North China University of Water Resources and Electric Power,
Zhengzhou 450046,
China
E-mail: *wangwen1621@163.com*;
wangwenchuan@ncwu.edu.cn

Kwok-wing Chau
Department of Civil and Environmental Engineering,
The Hong Kong Polytechnic University,
Hung Hom, Kowloon, Hong Kong,
China

Chang-jun Liu
China Institute of Water Resources and Hydropower Research,
Beijing 100038,
China

HIGHLIGHTS

- Propose a geomorphic unit hydrograph based on the principle of energy conversion.
- Develop a distributed flood-forecasting model using the proposed geomorphic unit hydrograph.
- The process of parameter determination of the developed model is very simple.
- The velocity distribution obtained from the analysis is reasonable.
- The developed hydrological model has a significant improvement in flood forecasting accuracy.

INTRODUCTION

Floods of medium and small catchments are among the most costly natural disasters all around the world, posing serious risk of loss of life, physical injury, damage to

infrastructure and disruption of economic and social activities (Shi *et al.* 2016). Last decades showed a steady increase of damages due to flooding, which highlighted the need of developing effective measures to reduce flood event impacts (Barbetta *et al.* 2018). Conceptual rainfall-runoff (CRR) models have become a basic tool for flood forecasting and become increasingly important for catchment basin

management (Xu *et al.* 2013). However, accurate flood prediction in mountainous watersheds remains a significant challenge for flood-forecasting models. In order to overcome this challenge, a good knowledge of the relationship between rainfall and runoff is entailed. A unit hydrograph is a common method in flood estimation, which is not only applied in peak flow estimation but also in the creation of complicated flood hydrographs (Khaleghi *et al.* 2011) and has been widely used in rainfall-runoff computation since it was proposed by Sherman (1932). Clark (1945) combined the two concepts of the isochrone method and linear reservoir to establish the instantaneous unit hydrograph. Although the Clark unit hydrograph can be a very valuable technique in flood hydrology, the lack of appropriate techniques to estimate the storage coefficient-*R* for ungagged watersheds has diminished the application and utility of this technique (Sabol 1988).

Obviously, there is a close relationship between the hydrological response of a river basin and its geomorphologic characteristics. Since Rodríguez-Iturbe & Valdés (1979) established the geomorphic instantaneous unit hydrograph theory (GIUH) by combining the initial probability of raindrop falling with the period transfer probability, there have been many attempts to propose an Instantaneous Unit Hydrograph that incorporated the geomorphological properties of the watershed (Gupta *et al.* 1980; Rodríguez-Iturbe *et al.* 1982; Agirre *et al.* 2005; Goñi *et al.* 2019). Agnese *et al.* (1988) derived the time scale of a GUIH from an effective stream flow velocity of the highest-order stream and the spatial distribution of velocity throughout the stream network. van der Tak & Bras (1990) incorporated hillslope effects into the gamma GIUH model by assuming that the hillslope travel distance in an area of a given order is approximated by the inverse of twice the local drainage density and introducing a hillslope velocity term. Cudennec *et al.* (2004) investigated the geomorphologic aspect of the unit hydrograph concept and concluded that the use of geomorphologic parameters explained the unit hydrograph and geomorphologic unit hydrograph theories.

Rosso (1984) combined the Nash model with geomorphic parameters based on the Horton Strahler river classification method and analyzed the GIUH by fitting the probability density distribution function of the flow concentration time. This method required computing the average velocity of the basin

flow concentration. For areas without sufficient data, the empirical formula proposed by Kirshen & Bras (1983) could be used to estimate the average convergence speed of a basin with the basin area, average rainfall intensity, river gradient, average river width and roughness. In order to reveal the spatially distributed nature of watershed properties, Maidment *et al.* (1996) proposed the concept of distributed spatial velocity field and analyzed the unit hydrograph by computing the spatial distribution of velocity. Tan *et al.* (2018) and Munoth & Goyal (2019) pointed out that when a digital elevation model (DEM) was used to divide sub-basins, DEM resolution and watershed threshold would have a greater impact on geomorphic parameters. Therefore, when using this method to build geomorphic unit hydrograph, it was necessary to analyze and demonstrate the applicability of DEM resolution and watershed division threshold. Kong & Guo (2019) studied the influence of rain intensity on velocity based on the Soil Conservation Service (SCS) velocity formula and proposed a time-varying distributed unit hydrograph computation method. These methods were based on geomorphic parameters.

With the continuous development and improvement, the construction of a geomorphic unit hydrograph based on the spatial velocity field has become a practical technology suitable for the flow concentration computation in ungauged basins. However, it is difficult to get a reasonable velocity distribution if only a single factor is considered. When considering multiple factors to estimate the velocity, it suffers from the limitation that the influence weight and parameter value of each factor are determined. In a flat area, there will be many grids with a slope of 0, which need to be treated with a special method. In fact, the transformation from gravitational potential energy to kinetic energy is the root cause of water flow. In the process of transformation, energy will be lost due to terrain, soil, vegetation, river diversion, water conservancy engineering and other factors.

The objective of this paper is to develop a method of constructing GIUH with clear physical meaning and study a method of determining the value of parameters. Based on this method, the distributed flood-forecasting model of Lianyuan Basin in China is established. In the proposed hydrological model, the spatial velocity field and the instantaneous unit hydrograph can be extracted based on the principle of energy conversion. It has many

advantages as mentioned below. Firstly, only one parameter of the model needs to be determined and the process of parameter determination is very simple. Secondly, the error caused by the gradient of 0 in the flat area is avoided and the velocity distribution obtained from the analysis is reasonable. Finally, the velocity results can be used for the simulation of both slope and river network flow concentration, which can ensure the consistency of flow concentration computation to a certain extent and reduce the influence of watershed threshold on model parameters when subwatershed is divided.

The paper is organized as follows: Section 'Methodology' describes the methodology proposed for the area rainfall calculation and runoff generation model and presents the flow concentration model in this study. Section 'Case study' gives details on the selected case study and model evaluation criteria. Section 'Results' presents and discusses the results obtained through the proposed methodology. Finally, we provide the conclusions of this work in the last section.

METHODOLOGY

Areal rainfall computation

The areal rainfall is computed by an inverse distance square (IDS) model. It can be approximately considered that the rainfall distribution in the basin is uniform because the area of sub-basin is very small. The result of the interpolation of the central point of the subwatershed is taken as the areal rainfall of the subwatershed.

IDS takes the distance between the interpolation point and a sample point as a weight. A sample point near the interpolation point has a greater weight, which is inversely proportional to the distance. It can be expressed as:

$$Z = \left(\sum_{i=1}^{n} \frac{1}{(D_i)^p} Z_i \right) / \sum_{i=1}^{n} \frac{1}{(D_i)^p} \tag{1}$$

where Z is the estimated value of the interpolation point, Z_i is the measured sample value, n is the number of measured samples involved in the computation, D_i is the distance

between the interpolation point and the ith station, p is the power of the distance, which significantly affects the interpolation results, and its selection standard is the minimum average absolute error. When p is taken as 0, the weights of all sample points are equal, and the method degenerates to an arithmetic mean model. When p is infinite, the result is approximately equal to the value of the nearest sample point, and the method is equivalent to the Voronoi model. In practical application, p is usually taken as 2 under the IDS model, which is the method adopted in this paper.

Runoff generation model

The Xinanjiang model is adopted for runoff generation computation. It is a CRR model with distributed parameters (Wang et al. 2012), which was developed by Zhao et al. (1980) and has been successfully and widely applied to the humid and semi-humid regions of China for flood forecasting (Zhao 1992). The model computes the basin evaporation and emission according to a three-layer evaporation and emission model. The total runoff produced by rainfall is computed according to the concept of full storage and runoff yield, and the influence of uneven underlying surface on the runoff yield area is considered by the water storage curve of the basin. In the aspect of runoff component division, according to the runoff production theory of 'hillside hydrology', the total runoff is divided into saturated surface runoff, soil water runoff and groundwater runoff by a free water storage reservoir with limited volume, measuring hole and bottom hole. For detailed descriptions and explanations of the Xinanjiang model, refer to Zhao (1992). The model structure is shown in Figure 1. It has 13 parameters and their physical descriptions are listed in Table 1. The value of each parameter is usually within certain ranges according to physical and mathematical constraints, information about watershed characteristics and from modelling experiences (Wang et al. 2012).

Flow concentration model

The concentration model is composed of two parts: the overland flow concentration and the river network flow
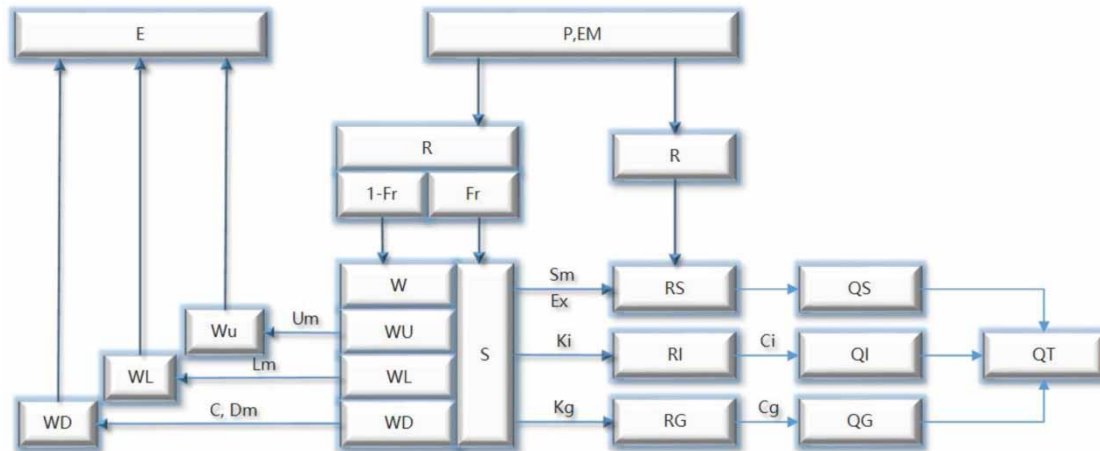
Figure 1 | Computation flow of the Xinanjiang model.

Table 1 | Physical meanings and units of Xinanjiang model parameters

	Parameter	Physical description	Unit
		Runoff generating parameter	
1	K	Ratio of potential evapotranspiration to pan evaporation	–
2	U_m	Averaged soil moisture storage capacity of the upper layer	mm
3	L_m	Averaged soil moisture storage capacity of the lower layer	mm
4	D_m	Averaged soil moisture storage capacity of the deep layer	mm
5	C	Coefficient of the deep layer that depends on the proportion of the basin area covered by vegetation with deep roots	–
6	B	Exponential parameter with a single parabolic curve, which represents the nonuniformity of the spatial distribution of the soil moisture storage capacity over the catchment	–
7	I_m	Percentage of impervious and saturated areas in the catchment	–
		Runoff routing parameter	
8	S_m	Areal mean free water capacity of the surface soil layer, which represents the maximum possible deficit of free water storage	mm
9	E_x	Exponent of the free water capacity curve influencing the development of the saturated area	–
10	K_g	Outflow coefficients of the free water storage to groundwater relationships	–
11	K_i	Outflow coefficients of the free water storage to interflow relationships	–
12	C_i	Recession constants of the lower interflow storage	–
13	C_g	Recession constants of the groundwater storage	–

concentration. The overland flow concentration denotes the process of net rain gathering along the slope to the river channel, and the river network concentration means that the flow converges to the downstream along all levels of river channels. The flow concentration time mentioned below denotes the time required for a water particle at any position in the basin to flow to the outlet section of the basin.

Overland flow concentration

A unit hydrograph is used to compute the runoff concentration according to the convolution formula.

$$Q_t = \sum_{i=1}^{m} I_i q_{t-i+1} (1 \leq t - i + 1 \leq m) \tag{2}$$

where m is the number of net rain periods, I is the average net rain period and q is the discharge of geomorphic unit hydrograph period.

According to D8 algorithm (Fairfield & Leymarie 1991), a water particle in a grid is assumed to flow to the adjacent grid in the direction of the maximum gradient in DEM. Figure 2(a) shows the elevation of each grid. Figure 2(b) displays the flow direction of each grid, in which water particles in any grid flow to its lowest adjacent grid, and thus, the flow concentration routes of each grid can be determined. The flow routes from a grid along the flow direction to the outlet of the basin are illustrated in Figure 2(c).

According to the size of each grid and the flow velocity in the grid, the detention time of water particles in each grid can be computed by the following formula:

$$\Delta\tau = L/v \quad \text{or} \quad \Delta\tau = \sqrt{2}L/v \tag{3}$$

where L is the length of the edge of the mesh converted to the actual distance and v is the flow velocity in the grid. Along the flow concentration route, the flow concentration time from each grid to the outlet of the drainage basin can be computed by the following formula:

$$\tau = \sum_{i=1}^{m} \Delta\tau_i \tag{4}$$

where m is the number of grids on the flow concentration route. Since the area of each grid is known, the drainage area corresponding to different flow concentration times can be computed, so as to obtain the flow concentration

time area relationship and compute the unit hydrograph according to the method in Kong *et al.* (2007).

The key point of geomorphic unit hydrograph computation is to estimate the velocity in the grid. The commonly used estimation methods are as follows (Maidment *et al.* 1996; Kang *et al.* 2006; Song *et al.* 2010):

$$v = aS^{1/2} \tag{5}$$

$$v = aS^b A^c \tag{6}$$

$$v = aS^b h^d \tag{7}$$

$$v = aS^b A^c i^d \tag{8}$$

where S is the slope of two adjacent grid points, A is the grid catchment area, h is the net rainfall of the unit grid, i is the net rainfall intensity and a, b, c, d are some parameters, where parameter a summarizes the combined effect of all other factors not described in the equations.

In fact, the fundamental cause of flood flow is the transformation of gravitational potential energy to kinetic energy. For any grid in the basin, assuming that the gravitational potential energy of rainfall falling on the basin is completely converted into kinetic energy without energy loss, then the kinetic energy of water particles flowing through the grid point satisfies the following formula:

$$E_{\text{ideal}} = \sum_{i=1}^{n} E_p = nmgH_{\text{Avg}} \tag{9}$$

where E_{ideal} is the total kinetic energy of flow in the grid under the ideal conditions; n is the total number of grids
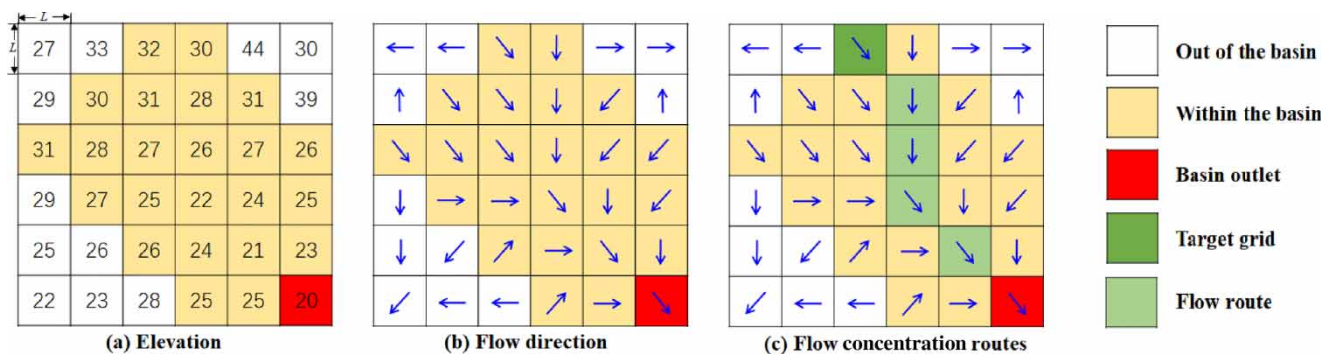

Figure 2 │ Flow direction and flow concentration routes.

in the basin upstream of the target grid (including the target grid); E_p is the gravitational potential energy of each upstream grid relative to the target grid; m is the mass of unit net rain in the grid; g is the gravity acceleration and H_{Avg} is the average elevation difference between all upstream grids and the target grid.

Due to the influence of topography, soil, vegetation, river diversion and hydraulic structures, the energy of water flow is gradually lost during the movement. The ratio of gravitational potential energy to kinetic energy is denoted by energy coefficient μ. According to the kinetic energy formula, the following formula is derived:

$$E_k = \mu E_{ideal} = \frac{1}{2}nmv^2 \tag{10}$$

where E_k is the kinetic energy of the flow from the target grid. The following equation is obtained by combining Equations (9) and (10):

$$v = \sqrt{2\mu g H_{Avg}} \tag{11}$$

For the grid on the watershed, the kinetic energy of the flow velocity is completely transformed from the gravitational potential energy, and the energy loss is mainly caused by the surface friction. Referring to the force of rigid body motion on the slope surface, the frictional force is directly proportional to the decomposition force of gravity in the vertical direction of the slope when the frictional coefficient is constant. When the slope is steeper, the supporting and frictional forces are smaller, and the speed is faster; when the slope is more gentle, the supporting and frictional forces are larger, and the speed is slower. Let $\mu = \mu'\sin(\theta/2)$, and rewrite Equation (11) as follows:

$$v = \sqrt{2\mu'\sin\frac{\theta}{2}g\Delta h} \tag{12}$$

where μ' is the energy residual coefficient, θ is the slope angle of the grid outflow direction and Δh is the elevation difference between the target grid and the outflow grid. For grids that are not on the watershed, the kinetic energy of water flow comes from two parts, one is the kinetic energy of the inflow grids,

and the other is the gravitational potential energy difference between the target grid and the outflow grid. The energy equation is as follows:

$$E_k = \sum_{i=1}^{N} E_i + \mu'\sin\frac{\theta}{2}nmg\Delta h \tag{13}$$

where N is the number of inflow grids of the target grid. The following direct equation of v can be obtained by combining Equations (10) and (13):

$$v = \sqrt{\frac{2\mu'\sin\dfrac{\theta}{2}ng\Delta h + \displaystyle\sum_{k=1}^{N} n_k v_k^2}{n}} \tag{14}$$

The following equation is equivalent to Equation (14)

$$v = \sqrt{\frac{2\mu'g \displaystyle\sum_{k=1}^{n} \sin\dfrac{\theta_k}{2}n_k\Delta h_k}{n}} \tag{15}$$

River network flow concentration

The Muskingum model is used for river network flow concentration, Muskingum equation is derived from the joint solution of water balance equation and Muskingum channel storage curve equation. The discharge at the river outlet can be computed according to the following equation:

$$Q_t = C_0 I_t + C_1 I_{t-1} + C_2 Q_{t-1} \tag{16}$$

where I_{t-1} and Q_{t-1} are the inflow and outflow of the channel at the beginning of the simulation, respectively. I_t and Q_t are the inflow and outflow of the channel at the end of the simulation, respectively. C_0, C_1 and C_2 are the parameters of the simulation and they can be determined by the following formula:

$$C_0 = \frac{\frac{1}{2}dt - Kx}{K - Kx + \frac{1}{2}dt} \tag{17a}$$

$$C_1 = \frac{\frac{1}{2}dt + Kx}{K - Kx + \frac{1}{2}dt} \tag{17b}$$

$$C_2 = \frac{K - Kx - \frac{1}{2}dt}{K - Kx + \frac{1}{2}dt} \tag{17c}$$

where dt is the time step of the simulation. In order to determine the parameter K, the wave velocity must be computed first. The spatial velocity field is used to compute the average velocity v, and a flow equation (Todini 2007) is used to compute the wave velocity of flood C.

$$C = \lambda v \tag{18}$$

where λ is the conversion coefficient. According to Tewolde & Smithers (2006), λ for rectangular n, parabola and triangle sections are taken as 5/3, 13/9 and 4/3, respectively.

The following formula is used to compute the propagation time of flood wave in the reach:

$$K = \frac{L}{3,600C} \tag{19}$$

The computation of x is given by Song et al. (2011)

$$x = \frac{1}{2} - \frac{n^{0.6}Q^{0.3}}{5.14\lambda J^{1.3}L} \tag{20}$$

where L is the length of the reach, n is the roughness, Q is the average of the maximum and minimum flow values in the inflow process and J is the gradient of the reach.

CASE STUDY

Study area and data

As shown in Figure 3, the study area is located in Hunan province of southern China and is the source of Lianshui, which is one of the tributary rivers in the Xiangjiang River. It originates in the south of Guanyin Mountain and the river flows through Lianyuan City from southwest to northeast. The catchment area of the basin is $160\ km^2$ with an average slope of 25.2%. The longest flow concentration route is 25.7 km. The average elevation of the basin is 268 m, and the maximum drop is 658 m. The soil in the basin is mainly sand clay on the hillside and clay loam on the riverside. The vegetation distribution consists of 60% of farmland and 40% of forest. Lianyuan Basin is located in the mid subtropical continental monsoon humid climate area, with the annual average precipitation of 1377.1 mm and 45% of the total rainfall falls between April and June.

The study area is divided into 11 sub-basin units by DEM data of $25\ m \times 25\ m$ resolution, including 256,000 grids. There are five rain gauging stations and one hydrological station in the study area. The rainfall weights of each rain gauging station computed by IDS for each sub-basin are listed in Table 2. A total of 29 historical floods between 1979 and 2006 are employed to calibrate the model parameters while 10 floods between 2010 and 2017 are utilized to verify these parameters. The time step in the model simulation is half an hour.

Evaluation criteria

To evaluate the suitability of the proposed model for the studied basin, three criteria are chosen to analyze the degree of goodness of fit. These criteria are Root Mean Square Error (RMSE), Nash–Sutcliffe Coefficient of Efficiency (NSCE) and three statistical ratios of acceptable criteria relative to the peak discharge, peak time and total runoff volume, which are introduced as follows:

In general, the criterion most commonly used in the literature has been RMSE in evaluating streamflows (Boyle et al. 2000; Cooper et al. 2007; Wang et al. 2012; Xu et al. 2013):

$$\text{RMSE} = \sqrt{\frac{1}{N}\sum_{i=1}^{N}(Q_s(i) - Q_0(i))^2} \tag{21}$$

where $Q_0(i)$ and $Q_s(i)$ are the measured and simulated runoff or corresponding runoff, respectively, and N is the number of data points involved.
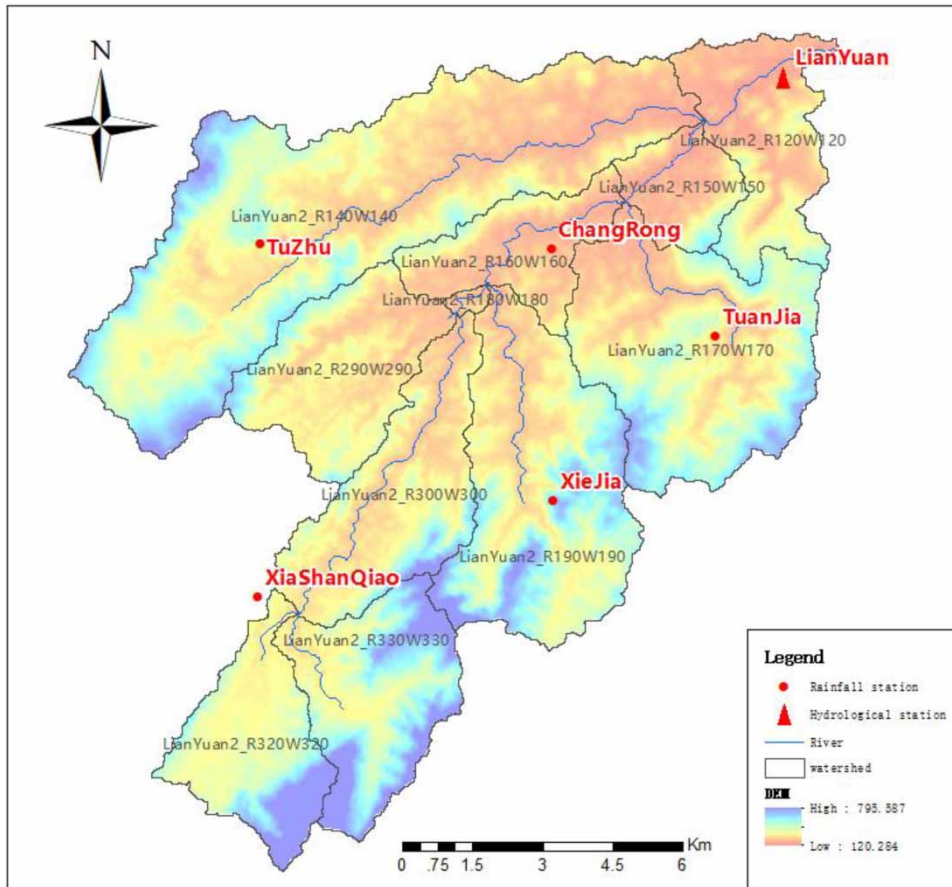
Figure 3 │ Schematic diagram of Lianyuan River Basin.

Table 2 │ Rainfall weights for each sub-basin in the study area

Sub-basin	Weight of rainfall station					
	LianYuan	XiaShanQiao	XieJia	ChangRong	TuanJia	TuZhu
LianYuan2_R120W120	0.881	0.005	0.013	0.041	0.051	0.009
LianYuan2_R140W140	0.039	0.048	0.058	0.182	0.055	0.618
LianYuan2_R150W150	0.349	0.018	0.052	0.299	0.248	0.034
LianYuan2_R160W160	0.015	0.007	0.018	0.913	0.030	0.019
LianYuan2_R170W170	0.003	0.001	0.004	0.007	0.984	0.001
LianYuan2_R180W180	0.037	0.036	0.091	0.642	0.090	0.104
LianYuan2_R190W190	0.007	0.014	0.907	0.029	0.031	0.011
LianYuan2_R290W290	0.034	0.136	0.132	0.164	0.068	0.466
LianYuan2_R300W300	0.031	0.270	0.368	0.123	0.081	0.128
LianYuan2_R320W320	0.019	0.748	0.097	0.042	0.037	0.058
LianYuan2_R330W330	0.025	0.572	0.217	0.061	0.058	0.066

The NSCE is a well-known performance criteria (Nash & Sutcliffe 1970), which is defined as:

$$NSCE = 1 - \frac{\sum_{i=1}^{N} (Q_s(i) - Q_0(i))^2}{\sum_{i=1}^{N} (Q_0(i) - \bar{Q})^2} \qquad (22)$$

where $\bar{Q}$ is the mean value of the measured processes.

According to the national criteria for flood forecasting in China (National Center of Hydrological Information 2000), in the calibrated and verified historical flood events, it is qualified if the error of peak discharge or total runoff is less than 20%, and the error of peak time is less than one computation step or 1 h. The qualified rate is computed by the following formula:

$$QR = \frac{n}{m} \qquad (23)$$

where QR is the qualified rate; n represents the total number of floods that satisfy the acceptable criteria relative to the peak discharge, peak time and total runoff volume, respectively; and m is the total number of the calibrated floods or validated ones. Three statistics ($QR_{peak\_discharge}$, QR_{peak_tm} and QR_{runoff}) are used to evaluate the effect of parameter calibration of a rainfall-runoff model (Wang *et al.* 2012; Xu *et al.* 2013).

The scheme is excellent when QR reaches 85%. The scheme is good when QR is greater than 75% and less than 85%. Otherwise, the results of the performances of parameter calibration are unsatisfactory for online flood forecasting.

RESULTS

29 floods are selected for model parameter calibration from 1979 to 2006. Table 3 gives the results of parameter calibration. According to three statistical ratios of acceptable national criteria relative to the peak discharge, peak time and total runoff volume among the calibrated and validated historical flood events for flood forecasting in China, Table 4 presents the detailed results of statistics performance using calibrated parameters during the calibration for flood simulation. It indicates that the qualified quantity is 24 and the ratio of qualifying simulation is 82.76% relative to the error of peak discharge; the qualified quantity is 27 and the ratio of qualifying simulation is 93.1% relative to the error of peak time; and the qualified quantity is 25 and the ratio of qualifying simulation is 86.21% relative to the error of total runoff volume. Ten floods are used for validation from 2010 to 2017. Table 5 gives the detailed results of statistics performance using the calibrated parameters during the validation for flood forecasting. It shows that the qualified quantity is 9 and the ratio of qualifying simulation is 90.0% relative to the error of peak discharge; the qualified quantity is 10 and the ratio of qualifying simulation is 100% relative to the error of peak time; and the qualified quantity is 9 and the ratio of qualifying simulation is 90.0% relative to the error of total runoff volume.

In order to demonstrate the comparative performance of the proposed Distributed Model based on Spatially Distributed Velocity Field using Equation (14) (DMSDVF) in this study, the Distributed Model based on Slope and Net Rainfall Intensity using Equation (7) (DMSNR) and the lumped Xinanjiang model (LXM) are employed for comparison. The calibrating and validating datasets of the two models are the same as those of the proposed model. The parameters of the two employed models are set in accordance

Table 3 | Model parameter calibration results

Parameter	U_m (mm)	L_m (mm)	D_m (mm)	B	I_m	K	C	S_m (mm)
Value	10	40	15	0.15	0.01	0.9	0.15	30
Parameter	E_x	K_g	K_i	C_g	C_i	μ'		
Value	1.1	0.5	0.4	0.9	0.3	0.005		

Table 4 | Simulation results during calibration

Floods	Observed (m³/s)	Simulated (m³/s)	Percentage error (%)	Observed peak time (yyyy-mm-dd hh)	Simulated peak time (yyyy-mm-dd hh)	Error (number)	Total volume error (%)
19790627	115	91.4	−20.5	1979-06-27 15:00	1979-06-27 16:30	−1.5	15.7
19800812	108	103	−8.3	1980-08-12 08:00	1980-08-12 17:00	−9	12.8
19810407	114	109.3	−4.1	1981-04-07 07:30	1981-04-07 09:00	−1.5	−4.5
19820616	170	151.2	−11.1	1982-06-16 19:42	1982-06-16 17:30	2.2	7.1
19870512	109	149.2	36.9	1987-05-13 02:30	1987-05-13 03:00	−0.5	25.6
19880829	99.9	95.3	−4.6	1988-09-03 15:36	1988-09-03 15:30	0.1	18.1
19900607	108	128.5	19.0	1990-06-07 11:00	1990-06-07 09:00	2	16.3
19900615	185	154.9	−16.3	1990-06-15 15:00	1990-06-12 23:00	64	−5.6
19920322	130	133.1	2.4	1992-03-20 06:00	1992-03-20 06:00	0	1.4
19920516	172	158.4	11.3	1992-05-17 00:12	1992-05-16 23:30	0.7	11.5
19920615	109	102.2	−6.2	1992-06-15 12:00	1992-06-15 13:00	−1	−5.2
19920622	259	250.9	−3.1	1992-06-22 09:30	1992-06-22 09:30	0	1.9
19930704	162	134.6	−17.5	1993-07-04 20:00	1993-07-04 20:30	−0.5	−28.1
19930720	170	263.6	55.1	1993-07-20 10:00	1993-07-20 08:00	2	49.2
19940425	98	82.7	−15.6	1994-04-25 08:00	1994-04-25 08:00	0	−6.0
19940718	206	184.3	−10.5	1994-07-18 17:12	1994-07-18 17:30	−0.3	−4.4
19940905	129	178.2	38.1	1994-09-06 11:30	1994-09-06 11:30	0	13.7
19950701	423	401.5	−5.1	1995-06-30 12:12	1995-06-30 12:00	0.2	2.6
19960601	108	108.8	4.5	1996-06-01 13:42	1996-06-01 15:30	−1.8	0.0
19960717	140	128.1	−17.4	1996-07-18 08:00	1996-07-18 08:30	−0.5	−17.9
19980522	293	309.6	5.7	1998-05-22 09:00	1998-05-22 09:30	−0.5	−0.3
19980624	169	144.8	−14.3	1998-06-25 02:30	1998-06-25 03:30	−1	−9.8
19990716	97.6	94.3	−3.4	1999-07-17 12:00	1999-07-17 10:00	2	−23.0
20020818	140	115	−17.9	2002-08-19 18:18	2002-08-19 16:00	2.3	−17.0
20030516	109	92.9	−14.8	2003-05-16 12:00	2003-05-16 12:30	−0.5	−14.3
20030605	81.5	56.8	−30.3	2003-06-05 20:42	2003-06-05 22:00	−1.3	−19.7
20040515	206	186.7	−9.4	2004-05-15 16:12	2004-05-15 16:30	−0.3	−4.6
20050601	183	161.2	−11.9	2005-06-01 10:30	2005-06-01 11:30	−1	−13.2
20060411	108	118.8	10.0	2006-04-12 12:48	2006-04 − 12 13:30	−0.7	−2.3

Notes: The total number of floods is **29**, which are qualificatory relative to the error of peak discharge, is **24** and the ratio of qualifying simulation is **82.76%**, which are qualificatory relative to the error of peak time, is **27** and the ratio of qualifying simulation is **93.1%**, which are qualificatory relative to the error of total runoff volume, is **25** and the ratio of qualifying simulation is **86.21%**.

with the best performance based on the calibrating programme. The performance statistics of the three models are summarized in Table 6 according to the evaluation criteria. It can be observed from Table 6 that the proposed DMSDVF attains the best RMSE, NSCE, $QR_{peak\_discharge}$, QR_{peak_time} and QR_{runoff} statistics of 12.6, 0.858, 82.76%, 93.1% and 86.21%, respectively, during calibration and attains the best RMSE, NSCE, $QR_{peak\_discharge}$ and

QR_{peak_time} statistics of 11.3, 0.918, 90% and 100%, respectively, during validation. The results of this analysis indicate that the proposed model is able to obtain the best result in terms of different evaluation measures during the calibration phase; and except QR_{runoff} value, the proposed model is also able to obtain the best results in terms of other evaluation measures during the validation phase. The performances of the three models developed in this paper during the

Table 5 | Simulation results during validation

Floods	Observed (m³/s)	Simulated (m³/s)	Percentage error (%)	Observed peak time (yyyy-mm-dd hh)	Simulated peak time (yyyy-mm-dd hh)	Error (number)	Total volume error (%)
20100510	227	266	17.2	2010-05-13 15:35	2010-05-13 14:00	1.6	17.2
20100608	167	217.5	30.3	2010-06-08 16:00	2010-06-08 16:30	−0.5	20.0
20100622	205	213	3.9	2010-06-24 10:15	2010-06-24 10:30	−0.3	10.4
20110612	184	199.3	8.3	2011-06-15 06:35	2011-06-15 04:00	2.6	24.0
20120610	125	138.1	10.5	2012-06-11 05:15	2012-06-11 03:30	1.8	4.2
20140704	117	111.8	−4.4	2014-07-05 05:20	2014-07-05 05:00	0.3	−3.7
20150605	206	242.1	17.5	2015-06-08 16:10	2015-06-08 16:30	−0.3	17.0
20150619	241	275.3	14.2	2015-06-21 14:30	2015-06-21 15:00	−0.5	13.3
20160704	170	194.6	14.5	2016-07-04 00:30	2016-07-04 00:30	0	1.8
20170627	254	207.4	−18.4	2017-07-01 11:30	2017-07-01 12:30	−1	−3.0

Notes: The total number of floods is **10**, which are qualificatory relative to the error of peak discharge, is **9** and the ratio of qualifying simulation is **90.0%**, which are qualificatory relative to the error of peak time, is **10** and the ratio of qualifying simulation is **100%**, which are qualificatory relative to the error of total runoff volume, is **9** and the ratio of qualifying simulation is **90.0%**.

Table 6 | Comparison of statistical results of three methods

Model	Evaluation result during calibration					Evaluation result during validation				
	RMSE (m³/s)	NSCE	QR$_{peak\_discharge}$ (%)	QR$_{peak\_time}$ (%)	QR$_{runoff}$ (%)	RMSE (m³/s)	NSCE	QR$_{peak\_discharge}$ (%)	QR$_{peak\_time}$ (%)	QR$_{runoff}$ (%)
DMSDVF	12.6	0.858	82.76	93.1	86.21	11.3	0.918	90.0	100.0	90.0
DMSNR	14.3	0.804	48.3	93.1	55.2	11.7	0.910	90.0	80.0	100.0
LXM	15.0	0.792	65.5	79.3	58.6	13.5	0.887	40.0	90.0	80.0

calibration and validation periods in the studied site are shown in Figures 4 and 5.

DISCUSSION

In the process of model parameter calibration, the most important parameter of the Xinanjiang model is the areal mean free water capacity of the surface soil layer S_m, which controls the redistribution of the total runoff under the assumption of the surface soil layer as a reservoir. As such, it is divided into surface water, soil-free water and groundwater. This parameter can be determined by simulation of the secondary flood peak flow. Secondly, the parameters that should be concerned are K_g and K_i, C_g and C_i, which can be estimated by analyzing the duration

of flood recession and calibrated by simulating the recession curve. The other parameters of the Xinanjiang model are rather insensitive, which only have a weak impact on the local details of the flood simulation process.

There are few parameters in the concentration model, but they significantly affect the simulation results of peak discharge and peak time. The geomorphic unit hydrograph parameters in Equations (5)–(8) are mostly empirical parameters, which have no clear physical meaning and can only be determined by calibration. The improved geomorphic unit hydrograph model has only one parameter μ', which can be determined both by calibration and measurement.

In order to analyze the effect of different velocity formulas, we use the same runoff generation model and parameters, and use Equations (7) and (14) to generate
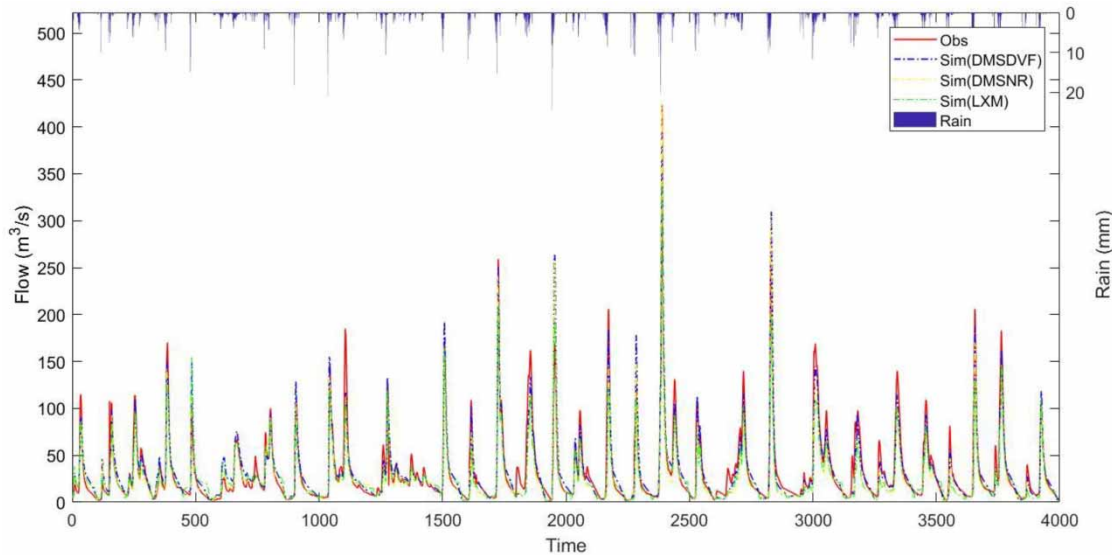
Figure 4 │ Comparison of observed and simulated hydrographs for 1979–2006 during calibration.
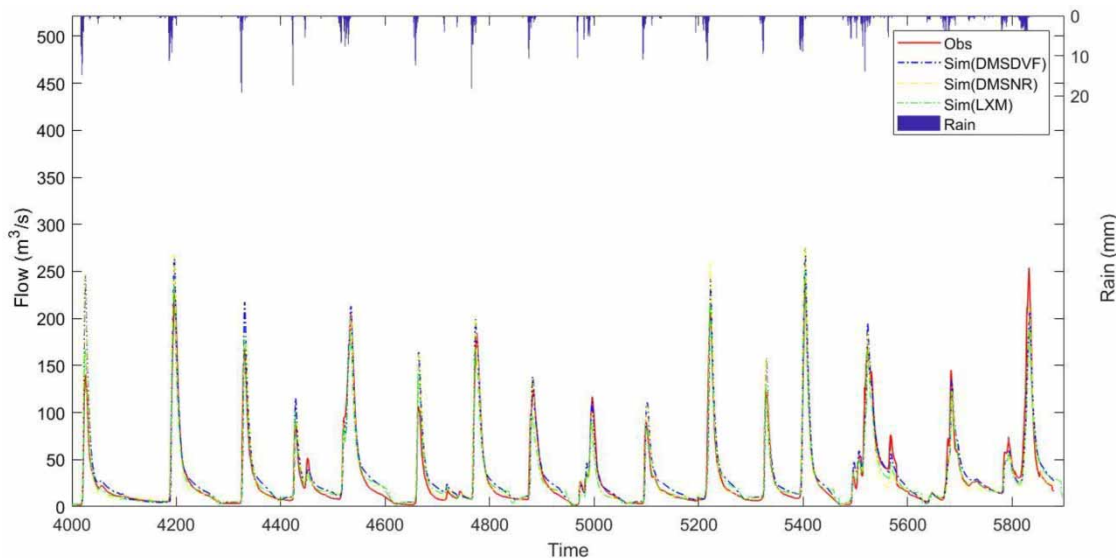

Figure 5 │ Comparison of observed and simulated hydrographs for 2010–2017 during validation.

different geomorphic unit hydrographs to simulate rainfall-runoff. As can be seen from the previous results, the simulation and forecasting results of the distributed model use Equation (14) based on the energy conversion method are obviously better than the other models. When Equation (7) is used to compute the flow velocity in the grid, the velocity is often considered to be positively correlated with slope and rainfall intensity, that is, under the same

conditions, the greater the slope and rainfall intensity, the faster the velocity will be. In this paper, parameter b of velocity formula is taken as 0.5 according to Maidment *et al.* (1996), parameter d is taken as 0.4 according to Li and Wen (1989) and the parameter a is calibrated as 0.5 based on the hydrological data. Although this method can also get good results, but its velocity distribution results are very different from the energy conversion method.

Figure 6(a) shows the velocity distribution computed by Equation (14) based on energy conversion. The velocity is generally 1–3 m/s on the steep slope, no more than 1 m/s on the flat land and mostly 1–2 m/s in the river channel. The velocity distribution considering slope and net rainfall intensity (in mm/h) is adopted by Equation (7) in Figure 6(b). It can be seen from Figure 6 that when the rain intensity is 1 mm/h, the velocity is generally 5–10 m/s on the steep slope, generally 2–5 m/s on the flat land and generally not more than 0.3 m/s in the river channel (many grid values are affected by a slope of 0). It is because the velocity under other rain intensities is in multiple ratios with the result under 1 mm/h with a ratio coefficient is i^d. When the rainfall intensity is 10 mm/h, the ratios are 2.51, 3.31 for 20 mm/h and 3.90 for 30 mm/h, respectively. From the numerical results, it can be seen that the velocity result is high on the slope and reasonable in the river by considering the slope and net rainfall intensity.

If $a = 0.5$, $b = 0.5$ and $d = 0.4$ are selected for the velocity estimation method of Equation (8) considering slope, rainfall intensity and catchment area, the velocity result close to Equation (7) can be obtained when parameter c tends to 0. When c is greater than 0, it can improve the situation of the velocity difference between slope land and river channel in Equation (7). The larger the catchment area is, the larger the velocity gain of the grid point is, but it will cause a very complicated calibration process.

It is easy to know from Equation (15) that velocity v is directly proportional to the square root of parameter μ' for any point in space, which is with a value of 15.38 m/s when $\mu' = 1$. The corresponding relationship between discharge and velocity is analyzed according to both the section measurement data and the stage–discharge relation of Lianyuan station. The average velocity of the section is computed to be 1.085 m/s by analyzing the total water volume and total kinetic energy of 39 floods. Table 7 presents the average velocity of each flood.

The result of μ' using Equation (24) is 0.00498, which is basically consistent with the calibration result $\mu' = 0.005$.

$$\mu' = \left(\frac{v}{v'}\right)^2 \tag{24}$$

The average elevation is 268 m and the outlet elevation is 137 m in the studied area. Assuming that the gravity potential energy is all converted into kinetic energy under
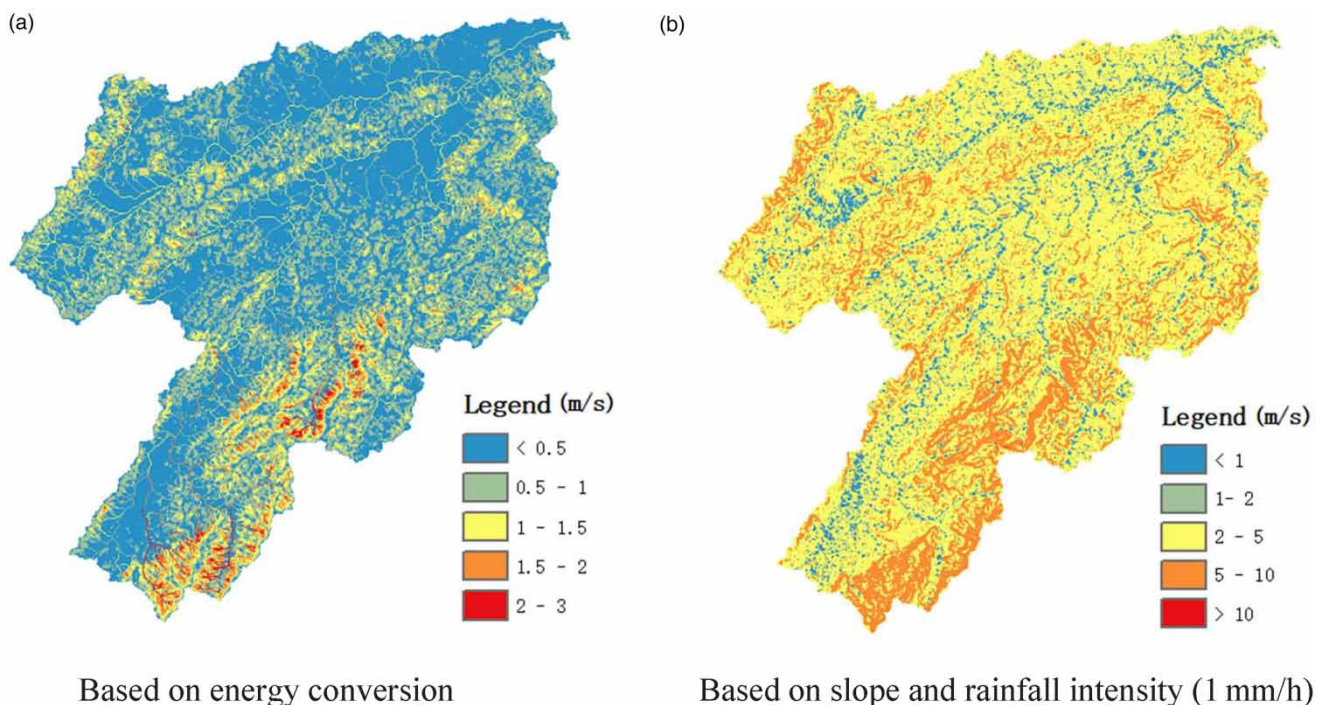

Figure 6 │ Spatial distribution of flow velocity.

Table 7 │ Average flow velocity of each flood

Floods	Flow peak (m³/s)	Total volume (10⁶ m³)	Average velocity (m/s)	Floods	Flow peak (m³/s)	Total volume (10⁶ m³)	Average velocity (m/s)
19790627	115	7.523	0.97	19980522	293	15.561	1.29
19800812	108	7.973	0.97	19980624	169	29.19	1.13
19810407	114	12.316	1.01	19990716	97.6	12.481	1.01
19820616	170	12.765	1.09	20020818	140	19.351	1.05
19870512	109	6.458	0.93	20030516	109	11.952	1.01
19880829	99.9	27.268	0.9	20030605	81.5	5.049	0.9
19900607	108	8.697	0.95	20040515	206	11.734	1.18
19900615	185	26.319	1.08	20050601	183	15.716	1.15
19920322	130	24.745	0.89	20060411	108	10.373	0.92
19920516	172	10.263	1.13	20100510	227	26.876	1.1
19920615	109	6.748	0.97	20100608	167	9.536	1.13
19920622	259	15.39	1.23	20100622	205	26.258	1.1
19930704	162	18.345	1.16	20110612	184	20.241	1.07
19930720	170	10.528	1.16	20120610	125	10.353	1.04
19940425	98	10.005	0.98	20140704	117	8.606	0.99
19940718	206	11.44	1.2	20150605	206	20.019	1.08
19940905	129	8.244	1.04	20150619	241	21.294	1.14
19950701	423	29.805	1.27	20160704	170	23.326	1.11
19960601	108	8.571	1.03	20170627	254	37.894	1.1
19960717	140	16.216	1.04				

an ideal condition, the average velocity of the outlet section of study area $v_{\text{ideal}} = \sqrt{2g\Delta H}$ is about 51 m/s. The energy conversion $\mu_{\text{efficiency}}$ can be computed by Equation (25):

$$\mu_{\text{efficiency}} = \left(\frac{v}{v_{\text{ideal}}}\right)^2 \tag{25}$$

When $\mu' = 0.005$, the energy conversion efficiency is 0.45‰, and it can be seen that a large amount of energy is lost in the process of water flow movement, denoting an inefficient conversion rate.

CONCLUSIONS

Hydrologic models are widely used tools for flood forecasting in the world, as the demand for accurate and reliable flood forecasts has increased in the management of water resources. This paper presents a new method for watershed concentration computation, which can be used to construct the hydrological model in areas without enough data. In order to simplify the computation, the residual energy coefficient is assumed to be constant in this paper and its value can be determined by calibration or measurement of the velocity. From the application point of view, the discretization of residual energy coefficient in spatial distribution is realized by measuring the velocity of different control nodes. As a matter of fact, it translates the flow concentration problem into a measurement problem (we can measure the flow velocity directly, or compute the flow velocity according to the hydraulic formula by using the measured channel section), and more precise flow concentration parameters can be obtained by more measurement data.

To demonstrate the applicability of the proposed method, a real-world catchment, Lianyuan River Basin is selected. For a 0.5 h time step, 29 historical floods in 28

years (1979–2006) are used for calibration, whereas 10 historical floods in 8 years (2010–2017) are utilized for verification. Three criteria are employed to evaluate the performances of the developed model. The result comparison indicates a significant improvement in the flood forecasting accuracy of the established distribution model, which uses energy conversion analysis of the geomorphic unit hydrograph. Hence, the velocity distribution computed by the energy conversion equation is more reasonable. The results of flow velocity can be used for the computation of both slope and river network flow concentration, which can ensure the consistency of flow concentration computation to a certain extent and reduce the influence of watershed threshold on model parameters in subwatershed division.

In terms of energy conversion efficiency, the ratio of gravitational potential energy to kinetic energy is very low in the process of flood movement, and most of it is converted into other forms of energy. There are many factors that affect the energy conversion. Future work should focus on further exploring the quantitative relationship between the energy coefficient and relevant influencing factors.

ACKNOWLEDGMENTS

DATA AVAILABILITY STATEMENT

Data cannot be made publicly available; readers should contact the corresponding author for details.

REFERENCES

Agirre, U., Goñi, M., López, J. J. & Gimena, F. N. 2005 Application of a unit hydrograph based on subwatershed division and comparison with Nash's instantaneous unit hydrograph. *CATENA* **64** (2), 321–332. https://doi.org/10.1016/j.catena.2005.08.013.

Agnese, C., D'Asaro, F. & Giordano, G. 1988 Estimation of the time scale of the geomorphologic instantaneous unit hydrograph from effective streamflow velocity. *Water Resources Research* **24** (7), 969–978. doi:10.1029/WR024i007p00969.

Barbetta, S., Coccia, G., Moramarco, T. & Todini, E. 2018 Real-time flood forecasting downstream river confluences using a Bayesian approach. *Journal of Hydrology* **565**, 516–523. https://doi.org/10.1016/j.jhydrol.2018.08.043.

Boyle, D. P., Gupta, H. V. & Sorooshian, S. 2000 Toward improved calibration of hydrologic models: combining the strengths of manual and automatic methods. *Water Resources Research* **36** (12), 3663–3674.

Clark, C. O. 1945 Storage and the unit hydrograph. *Transactions of the American Society of Civil Engineers* **110** (6), 1419–1446.

Cooper, V. A., Nguyen, V. T. V. & Nicell, J. A. 2007 Calibration of conceptual rainfall-runoff models using global optimisation methods with hydrologic process-based parameter constraints. *Journal of Hydrology* **334** (3–4), 455–466.

Cudennec, C., Fouad, Y., Sumarjo Gatot, I. & Duchesne, J. 2004 A geomorphological explanation of the unit hydrograph concept. *Hydrological Processes* **18** (4), 603–621. doi:10.1002/hyp.1368.

Fairfield, J. & Leymarie, P. 1991 Drainage networks from grid digital elevation models. *Water Resources Research* **27** (5), 709–717. doi:10.1029/90wr02658.

Goñi, M., López, J. J. & Gimena, F. N. 2019 Geomorphological instantaneous unit hydrograph model with distributed rainfall. *CATENA* **172**, 40–53. https://doi.org/10.1016/j.catena.2018.08.010.

Gupta, V. K., Waymire, E. & Wang, C. T. 1980 A representation of an instantaneous unit hydrograph from geomorphology. *Water Resources Research* **16** (5), 855–862. doi:10.1029/WR016i005p00855.

Kang, L., Wang, X.-L., Jiang, T.-B. & Guo, Y.-G. 2006 Watershed variable isochrones method based on DEM. *Shuili Xuebao/Journal of Hydraulic Engineering* **37** (1), 40–44.

Khaleghi, M. R., Gholami, V., Ghodusi, J. & Hosseini, H. 2011 Efficiency of the geomorphologic instantaneous unit hydrograph method in flood hydrograph simulation. *CATENA* **87** (2), 163–171. https://doi.org/10.1016/j.catena.2011.04.005.

Kirshen, D. M. & Bras, R. L. 1983 The linear channel and its effect on the geomorphologic IUH. *Journal of Hydrology* **65** (1), 175–208. https://doi.org/10.1016/0022-1694(83)90216-0.

Kong, F.-Z. & Guo, L. 2019 A method of deriving time-variant distributed unit hydrograph. *Shuikexue Jinzhan/Advances in Water Science* **30** (4), 477–484. doi:10.14042/j.cnki.32.1309.2019.04.003.

Kong, F.-Z., Li, Y. & Zhu, C.-X. 2007 Method deriving unit hydrographs based on area-time relation. *Zhongguo Kuangye Daxue Xuebao/Journal of China University of Mining and Technology* **36** (3), 356–359.

Li, Q. & Wen, K. 1989 Dynamic factor in GIUH formulae-study on the flow velocity. *Haihe Water Resources* **1**, 6–12.

Maidment, D. R., Olivera, F., Calver, A., Eatherall, A. & Fraczek, W. 1996 Unit hydrograph derived from a spatially distributed velocity field. *Hydrological Processes* **10** (6), 831–844. doi:10.1002/(sici)1099-1085(199606)10:6 < 831::Aid-hyp374 > 3.0.Co;2-n.

Munoth, P. & Goyal, R. 2019 Effects of DEM source, spatial resolution and drainage area threshold values on hydrological modeling. *Water Resources Management* **33** (9), 3303–3319. doi:10.1007/s11269-019-02303-x.

Nash, J. E. & Sutcliffe, J. V. 1970 River flow forecasting through conceptual models part I – a discussion of principles. *Journal of Hydrology* **10** (3), 282–290.

National Center of Hydrological Information 2000 *The National Criteria for Hydrological Forecasting*. Hydroelectric Press, Beijing.

Rodríguez-Iturbe, I. & Valdés, J. B. 1979 The geomorphologic structure of hydrologic response. *Water Resources Research* **15** (6), 1409–1420. doi:10.1029/WR015i006p01409.

Rodríguez-Iturbe, I., González-Sanabria, M. & Bras, R. L. 1982 A geomorphoclimatic theory of the instantaneous unit hydrograph. *Water Resources Research* **18** (4), 877–886. doi:10.1029/WR018i004p00877.

Rosso, R. 1984 Nash model relation to Horton order ratios. *Water Resources Research* **20** (7), 914–920. doi:10.1029/WR020i007p00914.

Sabol, G. V. 1988 Clark unit hydrograph and R-parameter estimation. *Journal of Hydraulic Engineering* **114** (1), 103–111. doi:10.1061/(ASCE)0733-9429(1988)114:1(103).

Sherman, L. K. 1932 Streamflow from rainfall by the unit-graph method. *Engineering News-Record* **108**, 501–505.

Shi, W., Li, L., Xia, J. & Gippel, C. J. 2016 A hydrological model modified for application to flood forecasting in medium and small-scale catchments. *Arabian Journal of Geosciences* **9** (4), 296. doi:10.1007/s12517-016-2314-0.

Song, X.-M., Kong, F.-Z. & Zhu, Z.-X. 2010 Method of concentration velocity considering rainfall intensity. *Water Resources and Power* **28** (8), 7–9. 75.

Song, X.-m., Kong, F.-z. & Zhu, Z.-x. 2011 Application of Muskingum routing method with variable parameters in ungauged basin. *Water Science and Engineering* **4** (1), 1–12. https://doi.org/10.3882/j.issn.1674-2370.2011.01.001.

Tan, M. L., Ramli, H. P. & Tam, T. H. 2018 Effect of DEM resolution, source, resampling technique and area threshold on SWAT outputs. *Water Resources Management* **32** (14), 4591–4606. doi:10.1007/s11269-018-2072-8.

Tewolde, M. & Smithers, J. 2006 Flood routing in ungauged catchments using Muskingum methods. *Water SA* **32** (3), 379–388.

Todini, E. 2007 A mass conservative and water storage consistent variable parameter Muskingum-Cunge approach. *Hydrology and Earth System Sciences* **11** (5), 1645–1659. doi:10.5194/hess-11-1645-2007.

van der Tak, L. D. & Bras, R. L. 1990 Incorporating hillslope effects into the geomorphologic instantaneous unit hydrograph. *Water Resources Research* **26** (10), 2393–2400. doi:10.1029/WR026i010p02393.

Wang, W.-C., Cheng, C.-T., Chau, K.-W. & Xu, D.-M. 2012 Calibration of Xinanjiang model parameters using hybrid genetic algorithm based fuzzy optimal model. *Journal of Hydroinformatics* **14** (3), 784–799. doi:10.2166/hydro.2011.027.

Xu, D.-m., Wang, W.-c., Chau, K.-w., Cheng, C.-t. & Chen, S.-y. 2013 Comparison of three global optimization algorithms for calibration of the Xinanjiang model parameters. *Journal of Hydroinformatics* **15** (1), 174–193. doi:10.2166/hydro.2012.053.

Zhao, R.-J. 1992 The Xinanjiang model applied in China. *Journal of Hydrology* **135** (1–4), 371–381.

Zhao, R. J., Zhang, Y. L. & Fang, L. R. 1980 The Xinanjiang model. In Hydrological Forecasting Proceeding Oxford Symposium. IASH, pp. 351–356.